

# Impact of Amazonian deforestation on atmospheric chemistry

Laurens Ganzeveld and Jos Lelieveld

Max-Planck Institute for Chemistry, Mainz, Germany

Received 2 December 2003; revised 28 January 2004; accepted 19 February 2004; published 17 March 2004.

[1] A single-column chemistry and climate model has been used to study the impact of deforestation in the Amazon Basin on atmospheric chemistry. Over deforested areas, daytime ozone deposition generally decreases strongly except when surface wetness decreases through reduced precipitation, whereas nocturnal soil deposition increases. The isoprene and soil nitric oxide emissions decrease although nitrogen oxide release to the atmosphere increases due to reduced canopy deposition. Deforestation also affects vertical transport causing substantial ozone and hydroxyl changes, also depending on soil moisture. The analysis shows that assessment of the impact of land cover and land use changes on atmospheric chemistry requires the development of explicitly coupled chemistry and meteorological models including surface trace gas exchanges, micro-meteorology and the hydrological cycle.

**INDEX TERMS:** 0315 Atmospheric Composition and Structure: Biosphere/atmosphere interactions; 0322 Atmospheric Composition and Structure: Constituent sources and sinks; 0368 Atmospheric Composition and Structure: Troposphere—constituent transport and chemistry; 1866 Hydrology: Soil moisture; 3322 Meteorology and Atmospheric Dynamics: Land/atmosphere interactions. **Citation:** Ganzeveld, L., and J. Lelieveld (2004), Impact of Amazonian deforestation on atmospheric chemistry, *Geophys. Res. Lett.*, 31, L06105, doi:10.1029/2003GL019205.

## 1. Introduction

[2] The terrestrial biosphere plays a crucial role in the atmospheric budget of many trace gases by acting as a sink through dry deposition of trace gases like ozone ( $O_3$ ) and sulfur dioxide ( $SO_2$ ). It is also a source of Volatile Organic Compounds (VOCs) whereas for a selection of gases, e.g., nitrogen oxides ( $NO$  and  $NO_2$ , collectively denoted as  $NO_x$ ), bi-directional exchanges can occur [e.g., Jacob and Bakwin, 1991]. Dry deposition and biogenic emissions are related to land cover and land use properties through their dependence on biogeochemical and biophysical properties. The parameters that control surface trace gas exchanges have been identified to develop models ranging from simple empirical models to explicit mechanistic models used to extrapolate site-scale observed fluxes in time and space, e.g., to arrive at global flux estimates. Examples are the inventories for biogenic VOC emissions by Guenther *et al.* [1995], soil-biogenic  $NO_x$  emissions by Yienger and Levy [1995] (hereafter referred to as YL95) and Potter *et al.* [1996] and dry deposition of  $O_3$ ,  $NO_x$  and sulfur oxides by Ganzeveld *et al.* [1998].

[3] These studies generally use databases that describe the global distribution of present-day land cover and land use characteristics. Of particular interest is the extent to which changes in land cover and land use, for example deforestation, will alter surface trace gas exchanges. Future climate change and increases in anthropogenic emissions could have significant effects on atmospheric chemistry and biogeochemistry. To study these complex interactions, process-based models, which explicitly simulate surface trace gas exchanges as a function of environmental parameters, are required. The global chemistry and climate model ECHAM includes an explicit representation of surface trace gas exchanges [Ganzeveld *et al.*, 2002], besides representations of processes such as convective and turbulent transport, micro-meteorology and the hydrological cycle.

[4] Here we present a study using a Single-Column Model (SCM) version of ECHAM4 [Roeckner *et al.*, 1996] in a so-called lagrangian mode by advecting the column from the Atlantic Ocean over the Amazon Basin to study the impact of deforestation on surface trace gas exchanges. We also include indirect effects on atmospheric chemistry through changes in the meteorology. The applied scenarios should not be interpreted as a prediction of future climate and atmospheric chemistry over Amazonia. Rather, the study has been performed to assess some of the complex interactions between, and the relative importance of meteorological and atmospheric chemistry processes related to land cover and land use changes.

## 2. Lagrangian Simulations With SCM

[5] The SCM contains an explicit representation of the surface trace gas exchange processes including a multi-layer atmosphere-biosphere trace gas exchange model [Ganzeveld *et al.*, 2002]. However, for practical reasons we have applied here the “big leaf” representation. To account for the canopy interactions, which are mostly relevant to  $NO_x$  exchanges, we use the YL95 Canopy Reduction Factor (CRF), which provides a good first-order estimate of canopy deposition [Ganzeveld *et al.*, 2002]. Dry deposition is calculated considering turbulent transport, diffusion and the surface uptake efficiency whereas biogenic  $NO$  and VOC emissions are calculated according to YL95 and Guenther *et al.* [1995], respectively. Surface parameters are inferred by combining satellite data and a high-resolution ecosystem database [Olson, 1992]. The gas-phase chemistry scheme considers the standard background methane oxidation reactions, as well as non-methane hydrocarbons including isoprene ( $C_5H_8$ ) and a selection of hydrocarbon oxidation products such as aldehydes and ketones [Roelofs and Lelieveld, 2000].

[6] In contrast to SCM simulations for a fixed geographical location, e.g., for model evaluation [Ganzeveld *et al.*,

**Table 1.** Characteristic Land Cover and Land Use Properties for Forest and Pasture

	Forest	Pasture
Leaf Area Index [ $\text{m}^2 \text{m}^{-2}$ ]	6–7	1.5
Canopy height [m]	15–30	0.5
Roughness [m]	1–2	0.05
$\text{C}_5\text{H}_8$ emis. fact. [ $\mu\text{g C g}^{-1} \text{hr}^{-1}$ ]	16	5
NO emis. fact. [ $\text{ng N m}^{-2} \text{s}^{-1}$ ]	2.6	0.36
Cultivation intensity [0–1]	0	0.2
Fertilizer use [ $\text{ng N m}^{-2} \text{s}^{-1}$ ]	0	13
Canopy Reduction Factor [0–1]	0.2–0.3	0.7

The range in the forest LAI, canopy height, roughness and CRF reflects the inferred range whereas for pasture those parameters have been prescribed.

2002], simulations can also be performed by advecting the column along prescribed transects. We applied realistic air mass trajectories from the northeastern coast of South America over the Amazon basin to the state of Rondonia, Brazil, following the trade winds. These trajectories indicate that there is only little wind shear with altitude in the Planetary Boundary Layer (PBL) and lower free troposphere, which is the domain of interest in this study. We show the results of a simulation, moving the column from its initial location at  $51^\circ\text{W}$ ,  $6^\circ\text{N}$  to  $61.4^\circ\text{W}$ ,  $10.3^\circ\text{S}$  within 3 days (28–30 March) using a time step of 60 seconds. We use initial temperature, moisture and wind speed profiles and surface properties such as soil moisture along the trajectory from the global 3-D ECHAM model.

[7] Two deforestation scenarios have been defined for comparison with the simulations for “present-day” land cover and land use properties. In one scenario, the “pasture” scenario, it is assumed that there is one continuous area in the middle of the Amazon ( $0^\circ$ – $5^\circ\text{S}$ ) where tropical rainforest is replaced by pastures. In a second scenario, the “patchy” scenario, we have assumed that at locations with a foliar density exceeding  $750 \text{ g m}^{-2}$ , the forest is replaced by pasture. This results in a total deforested area in the patchy scenario similar to that of the pasture scenario, used to assess the impact of the deforestation pattern on meteorology and atmospheric chemistry. For pasture an average Leaf Area Index (LAI) of 1.5, a canopy height of 0.5 m and a surface roughness of 0.05 m have been assumed. We selected the Olson [1992] ecosystem class “mild/hot farmlands and settlements” to represent the deforested areas, which determines the biogenic  $\text{C}_5\text{H}_8$  and NO emission factors, and included estimates of the cultivation intensity and fertilizer application according to Bouwman *et al.* [1995], as presented in Table 1.

### 3. Results

#### 3.1. Surface Trace Gas Exchanges

[8] Figure 1 shows the simulated ozone dry deposition velocities ( $V_{\text{dO}_3}$ ) and difference in LAI for the second and third day for the present-day and pasture scenario. In the pasture scenario the LAI decreases by about 75% compared to the present-day scenario for the second day, which results in a decrease in the daytime simulated  $V_{\text{dO}_3}$  of about  $0.6 \text{ cm s}^{-1}$  (60–70%). On the other hand, the decrease in LAI results in an increase in the nocturnal  $V_{\text{dO}_3}$  due to soil deposition. Despite a similar surface cover for the third day, there are differences up to  $0.7 \text{ cm s}^{-1}$  between the present-day and pasture scenario in the  $V_{\text{dO}_3}$ , mainly due to differ-

ences in the surface wetness. This also explains increases in the patchy scenario  $V_{\text{dO}_3}$  (not shown in Figure 1) compared to the present-day  $V_{\text{dO}_3}$  despite a 40% reduction in LAI.

[9] The impact of changes in surface wetness through changes in land cover on dry deposition is dependent on the assumptions about the uptake by wet vegetation. For example, the wet skin  $\text{SO}_2$  surface resistance of  $100 \text{ s m}^{-1}$ , which represents a highly variable uptake rate which could be as small as  $1 \text{ s m}^{-1}$  [Erismann *et al.*, 1994], is similar to the daytime dry vegetation uptake resistance. This results in a negligible change in the simulated  $V_{\text{dSO}_2}$  due to changes in surface wetness. On the other hand, the maximum formic acid dry deposition velocity, with an estimated negligible small wet surface resistance [Wesely, 1989], is  $4 \text{ cm s}^{-1}$  compared to a maximum  $V_{\text{dSO}_2}$  of  $1 \text{ cm s}^{-1}$  in the pasture scenario.

[10] The 3-day average fraction of wet surface in the deforestation scenarios is about 30–50% less compared to the present-day scenario. In addition, the LAI and surface roughness decrease by about 25%. Despite these relatively large changes in parameters that control dry deposition, the relative decrease in the average dry deposition velocities is only about 10%. This overall small decrease is partly explained by the compensating increased soil deposition especially for species with a soil uptake rate comparable to vegetation uptake, e.g.,  $\text{SO}_2$  and  $\text{O}_3$ .

[11] Furthermore we calculate an increase in the canopy-top  $\text{NO}_x$  fluxes from  $2.9 \text{ ngN m}^{-2} \text{s}^{-1}$  for undisturbed areas to  $5.7 \text{ ngN m}^{-2} \text{s}^{-1}$  for the deforested areas. Despite a significantly smaller emission factor for pasture compared to wet tropical forest soil the increase is partly explained by an increase in the CRF (which expresses a decrease in the canopy deposition), and enhancement of the emissions related to fertilizer use and a soil temperature increase. The difference between the maximum soil emission flux of about  $6 \text{ ngN m}^{-2} \text{s}^{-1}$  in the patchy scenario and  $8 \text{ ngN m}^{-2} \text{s}^{-1}$  in the pasture scenario largely reflects an increase in soil temperature of about 3K in the pasture scenario.

[12] Despite an increase in surface temperature, the deforestation results in a strong decrease in the isoprene emission fluxes due to a decrease in the emission factor as well as foliar density. The maximum forest  $\text{C}_5\text{H}_8$  emission flux of about  $12 \times 10^{15} \text{ molecules m}^{-2} \text{s}^{-1}$  decreases to about  $1.2 \times 10^{15} \text{ molecules m}^{-2} \text{s}^{-1}$  over pasture during the second day of the pasture scenario. In the patchy scenario the decrease in the foliar density and emission factor is partly compensated by an increase in the temperature over

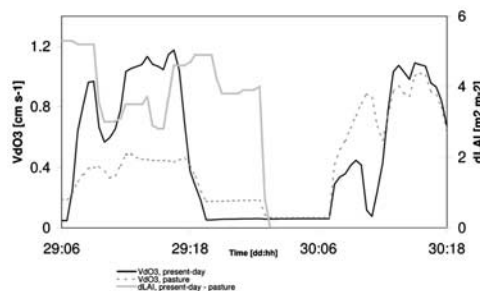


**Figure 1.** Ozone dry deposition velocities ( $V_{\text{dO}_3}$ ) and absolute differences in LAI (dLAI) for the present-day and pasture scenario for days 2–3.

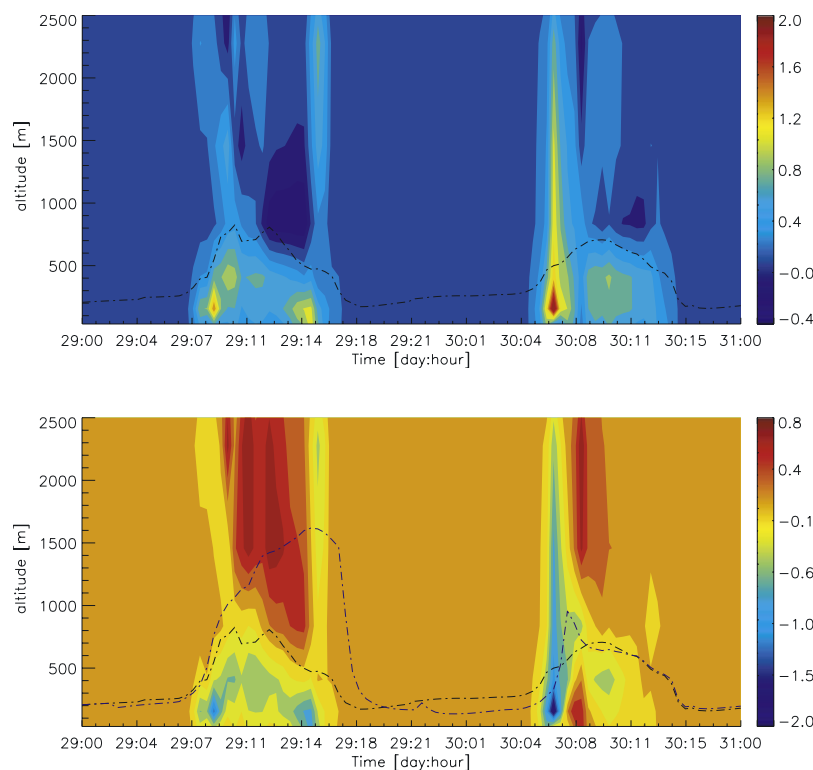


**Figure 2.** (a) Present-day ozone convective tendency ( $dO_{3-\text{conv}}$ ) [ $\text{ppbv hr}^{-1}$ ] as a function of altitude and time with dark blue colors indicating where convective transport provides a sink for ozone whereas other colors reflect a convective source of ozone and (b) change in  $dO_{3-\text{conv}}$  between the pasture and present-day scenario (calculated as pasture – present-day) where red colors indicate a decrease in the convective sink and other colors indicate a decrease in the convective source.

deforested areas resulting in an average decrease in the isoprene emission fluxes of about 30% over these areas. Interestingly, the integrated emission fluxes for the pasture and patchy scenarios are comparable suggesting that the deforestation pattern does not result in a significant change in the area average isoprene emission flux through non-linear temperature effects.

### 3.2. Meteorology and Atmospheric Chemistry

[13] The deforestation results in a decrease in evapotranspiration, humidity and cloud cover. In addition, there is an increase in the sensible heat flux, surface and air temperature and PBL depth. A key parameter that controls the energy partitioning is soil moisture by regulating stomatal exchange and consequently evapotranspiration. In our simulations we have not modified soil moisture although it may be expected that deforestation will affect soil moisture through changes in precipitation, rainfall interception and soil properties. To indicate the sensitivity of our analysis to soil moisture we have performed additional simulations where we reduced the pasture soil moisture to 50% of the field capacity (the maximum amount of water that can be held by a soil). Figure 2a and 2b show the present-day  $O_3$  convective tendency ( $dO_{3-\text{conv}}$ , which reflects the change in the ozone concentrations due to convection) up to 2500 m for day 2 and 3 and the change in  $dO_{3-\text{conv}}$  between the present-day and pasture scenarios, including reduced soil moisture. We calculate a maximum decrease in  $dO_{3-\text{conv}}$  of about  $1.8 \text{ ppbv hr}^{-1}$ , which is comparable to the absolute tendency of the present-day simulation. The decrease in

humidity is such that convective transport largely diminishes over the deforested area and also reduces over the forest during the third day. Also shown are the changes in the simulated PBL height for the two scenarios, with a maximum height for the present-day scenario of about 700 m whereas the PBL height for the deforestation scenario reaches an altitude of about 1700 m. This increase also reflects a more efficient dilution of species emitted from the surface.

[14] The average increase in the surface layer ozone concentration in response to deforestation is less than 2 ppbv, also due to the compensating effect of enhanced nocturnal and reduced daytime dry deposition, whereas slightly larger increases, associated with changes in the vertical transport, occur at higher altitudes.

[15] The large reduction in the isoprene emission fluxes results in a decrease in the daytime isoprene surface layer concentrations from about 5 ppbv over the forest to less than 1 ppbv over the pasture in the pasture scenario. This, combined with the ozone increase, partly explains the relative increase in the hydroxyl radical (OH) concentrations in excess of 50% in the PBL and free troposphere. Figures 3a and 3b show the present-day OH concentrations for day 2–3 up to 2500 m and the absolute difference between the pasture and present-day scenario OH concentrations (calculated as pasture minus present-day), respectively. The OH concentration is sensitive to the assumed soil moisture through its control of the evapotranspiration and thereby the humidity, cloud cover and consequently the photo-dissociation of ozone (through  $\text{H}_2\text{O} + \text{O} (^1\text{D}) \rightarrow$

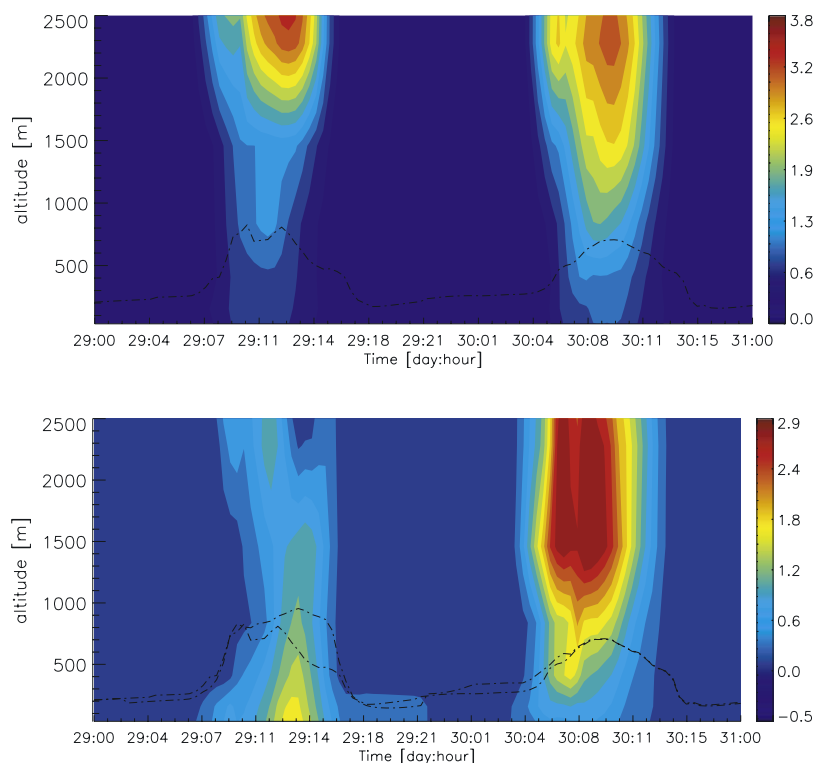


**Figure 3.** (a) Present-day OH concentrations [ $10^6$  molec.  $\text{cm}^{-3}$ ] as a function of altitude and time and (b) absolute difference between the pasture and present-day scenario (calculated as pasture-present-day) OH concentrations where all colors except of dark blue indicate an increase.

2OH). For example, the reduced soil moisture simulations for the patchy scenario show a 3-day average decrease in the tropospheric OH concentrations up to 5 km altitude of 10% with maximum changes in excess of 50%. These changes in OH concentrations mainly reflect changes in the photo-dissociation of ozone ( $\text{JO}_3$ ) dependent on the cloud-cover and the cloud vertical extent.  $\text{JO}_3$  decreases above and increases below a reduced cloud cover and vice versa. Interestingly, the decrease in soil moisture does not only induce substantial decreases but also increases in cloud cover from  $-75\%$  to  $+30\%$ , depending on, e.g., surface energy partitioning, the vertical structure of the atmosphere and the history of the air parcel; these aspects need further analysis with comprehensive models.

#### 4. Conclusions

[16] Our analysis of the impact of deforestation on atmospheric chemistry indicates that local and short-term changes in dry deposition velocities related to changes in surface cover parameters such as LAI and surface wetness are large, however, area average changes are relatively small. Nevertheless, quantification of the impact of changes in surface wetness on dry deposition is limited by the fact that uptake by water covering leaves is a poorly understood process, which is the main reason that constant wet surface uptake rates have been applied in our study.

[17] The use of constant empirical emission factors also limits the assessment of the impact of deforestation on biogenic emissions. The roles of parameters such as radiation, temperature and canopy deposition are included; however, the model does not explicitly include parameters

that regulate longer-term changes in soil N emissions, e.g., the nutrient status. Consequently, process-based models that explicitly consider the dependency of those parameters on biogeochemical and biophysical processes should be used for further evaluation of the impact of deforestation on soil N emissions [Ganzeveld *et al.*, 2004].

[18] A key parameter in our analysis is soil moisture, which largely controls the surface energy balance, dry deposition, vertical transport and cloud processes affecting photo-dissociation, and also wet deposition. Therefore, further analysis of the impact of deforestation on atmospheric chemistry should involve the long-term and large-scale impact of deforestation on soil moisture using global climate models like ECHAM.

[19] Our analysis suggests that deforestation has a large impact on atmospheric chemistry through changes in emissions, deposition and especially through changes in the meteorology and hydrological cycle. Consequently, quantitative assessment of the impact of land cover and land use changes on atmospheric chemistry will require the development of explicitly coupled chemistry and meteorological models that realistically represent surface trace gas exchanges, micro-meteorology and the hydrological cycle.

[20] **Acknowledgments.** We thank Erik van Meijgaard from the Royal Netherlands Meteorological Institute (KNMI) for making available the Single-Column Model with ECHAM4-physics.

#### References

Bouwman, A. F., and K. W. van der Hoek, *et al.* (1995), Uncertainties in the global source distribution of nitrous oxide, *J. Geophys. Res.*, **100**, 2785–2800.



- Erismann, J. W., A. Van Pul, and P. Wyers (1994), Parameterization of surface resistance for the quantification of atmospheric deposition of acidifying pollutants and ozone, *Atmos. Environ.*, **28**, 2595–2607.
- Ganzeveld, L., J. Lelieveld, and G.-J. Roelofs (1998), Dry deposition parameterization of sulfur oxides in a chemistry and general circulation, *J. Geophys. Res.*, **103**, 5679–5694.
- Ganzeveld, L., and J. Lelieveld, et al. (2002), Atmosphere-biosphere trace gas exchanges simulated with a single-column model, *J. Geophys. Res.*, **107**(D16), 4320, doi:10.1029/2001JD000684.
- Ganzeveld, L., C. Li, et al. (2004), Nitrogen emissions from soils, in *Emissions of Atmospheric Trace Compounds*, edited by C. Granier, P. Artaxo, and C. Reeves, 544 pp., Kluwer Academic Publishers, Dordrecht, The Netherlands, in press.
- Guenther, A., and C. Nicolas Hewitt, et al. (1995), A global model of natural volatile organic compound emissions, *J. Geophys. Res.*, **100**, 8873–8892.
- Jacob, D. J., and P. S. Bakwin (1991), Cycling of NO<sub>x</sub> in tropical forest canopies, in *Microbial production and consumption of greenhouse gases: Methane, nitrogen oxides and halomethanes*, edited by J. E. Rogers and W. B. Whitman, 237–253, American Soc. of Microbiology.
- Olson, J. (1992), World ecosystems (WE1. 4): Digital raster data on a 10 minute geographic 1080 × 2160 grid square, in *Global Ecosystem Database, Version 1. 0: DISC A*, edited by NOAA National Geophysical Data Center, Boulder, CO.
- Roeckner, E., K. Arpe, L. Bengtsson, M. Christoph, M. Claussen, L. Dümenil, M. Esch, M. Gjogetta, U. Schlese, and U. Schulzweida (1996), The atmospheric general circulation model ECHAM-4: Model description and simulation of the Present-day Climate, Report No. 218, Max-Planck-Institut für Meteorologie, Hamburg.
- Roelofs, G.-J., and J. Lelieveld (2000), Tropospheric ozone simulation with a chemistry-general circulation model: Influence of higher hydrocarbon chemistry, *J. Geophys. Res.*, **105**, 22,697–22,712.
- Potter, C. S., P. A. Matson, P. M. Vitousek, and E. Davidson (1996), Process modeling of controls on nitrogen trace gas emissions from soils worldwide, *J. Geophys. Res.*, **101**(D1), 1361–1377.
- Wesely, M. L. (1989), Parameterization of surface resistances to gaseous dry deposition in regional-scale numerical models, *Atmos. Environ.*, **23**, 1293–1304.
- Yienger, J. J., and H. Levy II (1995), Global inventory of soil-biogenic NO<sub>x</sub> emissions, *J. Geophys. Res.*, **100**, 11,447–11,464.
- 
- L. Ganzeveld and J. Lelieveld, Max-Planck Institute for Chemistry, Mainz, Germany. (ganzeveld@mpch-mainz.mpg.de)